



# TGF $\beta$ signalling pathway impacts brain metastases profiles in locally advanced colorectal cancer

Sven Jacob<sup>1</sup> · Ilja Balonov<sup>1</sup> · Vindi Jurinovic<sup>4</sup> · Christian Heiliger<sup>1</sup> · Tengis Tschaidse<sup>1</sup> · Jörg Kumbrink<sup>3</sup> · Thomas Kirchner<sup>3</sup> · Jens Werner<sup>1</sup> · Martin K. Angele<sup>1</sup> · Marlies Michl<sup>2</sup> · Jens Neumann<sup>3</sup>

Received: 20 September 2023 / Accepted: 2 February 2024  
© The Author(s) 2024

## Abstract

**Rationale** Colorectal Cancer (CRC) represents the third most common type of cancer in Germany and the second most common cancer-related cause of death worldwide. Distant metastases are still the main limit for patient survival. While liver metastases as well as peritoneal carcinomatosis can often either be resected or treated with systemic therapy, little options remain for brain metastases. Additionally, a number of studies has already investigated hepatic, peritoneal, pulmonary as well as continuing distant metastases in colorectal cancer. Yet, with respect to tumor biology and brain metastases, little is known so far.

**Material and methods** Two cohorts, M0 without distant spread and BRA with brain metastases were build. RNA was isolated from paraffin embedded specimen. Gene expression was performed by an RNA NanoString-Analysis using the nCounter® PanCancer Progression Panel by NanoString-Technologies (Hamburg, Germany). Results were analysed by principal component analysis, gene expression and pathway analysis using commonly available databases such as KEGG as benchmark for comparison.

**Results** We were able to determine a gene signature that provides a sophisticated group separation between M0 and BRA using principal component analysis. All genes with strong loading characteristics on principal component 1 were cross-referenced with the subsequently performed accurate gene set enrichment analysis (GSEA). The GSEA revealed a clear dysregulation of the TGF $\beta$  pathway in compared cohorts M0 and BRA. Interestingly, the targeted pathways analysis of the identified genes confirmed that in fact almost all strong loading genes of PC1 play a role in the TGF $\beta$  pathway.

**Conclusion** Our results suggest the TGF $\beta$  pathway as a crucial player in the development of brain metastases in primary CRC. In some types of colorectal cancer, downregulation of the TGF $\beta$  pathway might hinder primary colorectal cancer to metastasize to the nervous system. While the paradoxical functioning of the TGF $\beta$  pathway is still not fully understood, these shed light on yet another clinical implication of this complex pathway.

**Keywords** Colorectal cancer · Hematogenous spread · Brain metastasis · Pathway analysis · Gene signature · TGF $\beta$  signalling pathway influences CRC brain metastasis

---

Marlies Michl and Jens Neumann have contributed equally to the study.

---

✉ Jens Neumann  
jens.neumann@med.uni-muenchen.de

<sup>1</sup> Department of General, Visceral and Transplantation Surgery, University Hospital, LMU Munich, Munich, Germany

<sup>2</sup> Department of Medicine III, University Hospital, LMU Munich, Munich, Germany

<sup>3</sup> Institute of Pathology, Medical Faculty, Ludwig-Maximilians-University (LMU) Munich, Marchioninstr. 15, 81377 Munich, Germany

<sup>4</sup> The Institute for Medical Information Processing, Ludwig-Maximilians-University (LMU) Munich, Biometry, and Epidemiology, Munich, Germany

## Introduction

Colorectal Cancer (CRC) represents the third most common type of cancer in Germany and the second most common cancer-related cause of death worldwide. With more than 25% of CRC being diagnosed in distant metastatic state, one of the decisive factors for prognosis is the localization of distant metastases [1, 2]. Patients with liver metastases are often admissible for a curative approach. However, lacking possibilities of resection of metastases, which especially occurs in brain metastasis acts critically limiting for the prognosis [3]. Thus, it is crucial to understand the heterogeneous organotropism of CRC and its molecular background leading to brain metastases.

Although there are standardized algorithms for liver and lung metastases, patients with brain metastases (BRA) are relatively rare and hence present a lack of standardized screening and treatment. With an average incidence of up to 4%, the rare but drastic state of BRA demands the need to be identified in early diagnostic processes since median overall survival with BRA is limited to 2–9 months [1, 4]. The complex interaction between genetic variability in patients with CRC and organotropism for liver, lung and peritoneal metastasis has been described in detail [5, 6]. Regarding brain metastases, this is not the case. Besides a mutation in KRAS, no clinically relevant gene mutations as well as no molecular pathways have been delineated to predict brain metastases in the CRC [7]. However, in patients with brain metastases from similarly common disease such as breast cancer and prostate cancer, several genes and pathways have been described to comprise somatic and germline mutations [8]. Among these, the TGF $\beta$  signalling pathway seems to play a crucial role. Respectively, there is an urgent need of further diversified genetic elucidation of patients with CRC and BRA as well as deeper investigation of genes and pathways involved. This is even more important because the most sensitive detection tool, the MRI, is rarely indicated and stays costly in terms of time, financial and technical resources for the health system in relation to this comparably rare condition [1].

In an attempt to identify frequently mutated genes in primary CRC with BRA, this study investigates specimens of locally advanced primary CRC without distant spread in comparison to primary CRC specimens leading to brain metastases. In respect to the heterogeneous tumor biology of CRC, RNA NanoString analysis has been used to gain insights of differentially expressed gene. Principal component analysis, gene set enrichment analysis (GSEA) and pathway analysis from several widely used databases in both groups have been conducted. Furthermore, the results have been validated in corresponding data from the Kyoto Encyclopaedia of Genes and Genomes (KEGG).

## Material and methods

### Study population

Patients undergoing colorectal surgery at the Department of General, Visceral and Transplantation Surgery at the Ludwig-Maximilian University Hospital Munich (Munich, Germany) were registered in a prospectively maintained database. Retrospectively, the patients were identified for the study population from this database using a predefined study protocol that was designed to address the research question at hand.

Criteria for study population were:

- Confirmed diagnosis of colorectal carcinoma by pathology
- Exclusion when additional malignant diagnosis other than colorectal carcinoma
- Exclusion of patients missing formalin-fixed paraffin-embedded (FFPE) tissue of the primary tumor
- Exclusion of patients presenting with Lynch-Syndrom and other hereditary diseases
- Exclusion of patients lost to follow up in the first 5 years

All CRC in the database were staged and documented by a pathologist according to the 7th edition AJCC TNM criteria from 2018. Follow up was achieved by cross-sectional imaging and continuous patient visiting. For investigational purposes, patients with hepatic and peritoneal metastases were not included in the present analysis, thus twelve patients, six from each group with and without brain metastases, were randomly selected for further characterization. Primary tumor RNA was isolated from FFPE specimens via microdissection as described previously. The study was carried out according to the recommendations of the local ethics committee of the Medical Faculty of the Ludwig-Maximilians-University Munich, Germany, which approved the study with protocol no. 19-966.

### Gene expressions analysis

This panel includes 770 genes particularly associated with the appearance and progression of distant metastases [9, 10]. Gen Set Enrichment Analysis (GSEA) was conducted by the JAVA program 2021. Gene set permutations were conducted 1000 times for each evaluation analogue to risk profiles previously described in numerous studies from the TCGA and ARG. The gene expression profiles and corresponding clinical information, such as age, gender, TNM classification and localization of distant metastases were maintained in the data base at hand. The primary GSEA included the whole genome analysis and was

performed using the Broad Institute software. All values were compared to pathways from openly available databases: Reactome, Biocarta, Kyoto Encyclopedia of Genes and Genomes (KEGG), Gene Ontology (GO), Hallmark gene sets, oncogenic and immunologic signatures [11–13]. We adjusted all nominal p-values for multiple testing for each specific pathway data base with the Bonferoni-Holm method (q-value). P-values  $\leq 0.05$  and q-values  $\leq 0.25$  are assumed significant, p-values  $< 0.001$  were considered highly significant.

## Statistical analysis

Statistical calculation was conducted using SPSS Version 25.0 (PASW, SPSS Inc. Chicago, IL, USA), MetaboAnalyst Version 5.0 ([www.metaboanalyst.ca](http://www.metaboanalyst.ca)) and GraphPad Prism Version 9.1.2 (GraphPad Software, La Jolla, CA, USA). The data was presented as the mean for continuous variables and percentages for categorical variables. Associations and disparities were assessed by students t-test and a two-sided  $\chi^2$  tests. Unsupervised principal component analysis (PCA) was applied to identify gene clusters. Functional groups of genes have been merged in synopsis with the statistical results and pathway analysis respectively. Clinicopathological data were delineated using one-way analysis of variance (ANOVA) and Tukey's multiple comparisons test for multiple comparison correction. A two-sided p-value  $< 0.05$  was considered statistically significant. Parameters with missing data (e.g., adjuvant chemotherapy) were included in the multivariate analysis by adding the category "unknown" to the respective variable to prevent listwise exclusion of cases from further analysis.

## Results

### Clinicopathological parameters

A total of 12 patients have been included in the complete dataset, six in each group. Median age of patients was 72.5 years ( $\pm 1.5$  years) and the female to male ratio was seven female vs. five male patients. Regarding primary tumor location, there was no statistically significant difference between groups, the same applies to tumor grading. As defined per study protocol and confirmed by histology, all patients suffered from colorectal carcinoma. Likewise, every patient underwent systemic chemotherapy and resection. As expected, the difference in tumor stadium between M0 and

**Table 1** Clinicopathological parameters

Variable	M0 n (%)	BRA n (%)	p-value
Patients	6	6	
Medium age	71	74	0.72
Sex			
Female	4 (66.6)	3 (50.0)	0.75
Male	2 (33.4)	3 (50.0)	
Location of PT			
Right colon	2(33.3)	4 (66.7)	0.40
Left colon	4 (66.7)	2 (33.3)	
UICC			$< 0.05$
I	0 (0.0)	0 (0.0)	
II	0 (0.0)	0 (0.0)	
III	6 (100.0)	0 (0.0)	
IV	0 (0.0)	(100.0)	
Grading			
Low grade	3 (50.0)	3 (50.0)	0.99
High grade	3 (56.9)	3 (50.0)	
Chemotherapy			
Yes	6 (100.0)	6 (100.0)	$> 0.9$
No	0 (0.0)	0 (0.0)	0 (0.0)

Bra = brain metastases, M0 = no metastases

BRA was statistically significant with all patients in BRA being classified as UICC 4 (Tables 1 and 2).

## Gene expression

### Overall principal component analysis

At first, a PCA with 770 genes has been examined in order to identify principal components potentially indicating genes, which separate the cohorts BRA and M0. Kaiser–Meyer–Olkin Measure of Sampling Adequacy (KMO = 0.678 and Chi-quadrat (120) = 420,  $p < 0.02$ ) displays validity of the calculated principal component analysis. Principal component 1 explains 32.6% of variance. PC2 explains 20.1% of variance in given calculation. Further components tested did not add any additional value. The corresponding Scree plot in Fig. 1B shows five PCs with an Eigenvalue  $> 1$ . Each point in the plot delineates a tissue sample. However, principal component analysis did not show a relevant genetic separation. With no distinct elbow spot in the plot, further evaluation of given model does not indicate if a two-, three-, four- or five-factor analysis will facilitate an adequate result. In an S-plot, a group of genes have been identified to separate from the main group graphically. Reckoning of genes with notably low or high covariance, a further examination on significance will follow the previous analysis.

**Table 2** Mutational status

Sample	Group	KRAS	NRAS	BRAF	MSI	T	N	M	G
1	BRA	mut (Ex2)	wt	wt	MSS	3	1	1	3
2	BRA	mut (Ex2)	wt	wt	MSS	4	1	1	2
3	BRA	mut (Ex2)	wt	wt	MSS	4	2	1	3
4	BRA	wt	wt	mut	missing	3	2	1	2
5	BRA	wt	wt	wt	MSS	4	2	1	2
6	BRA	wt	wt	wt	MSS	3	2	1	2
7	M0	missing	missing	missing	missing	3	1	0	3
8	M0	wt	missing	wt	missing	3	2	0	3
9	M0	missing	wt	missing	MSS	3	1	0	3
10	M0	missing	missing	missing	missing	3	1	0	2
11	M0	wt	mut	missing	missing	3	2	0	2
12	M0	mut (Ex2)	fehlt	missing	missing	3	1	0	2

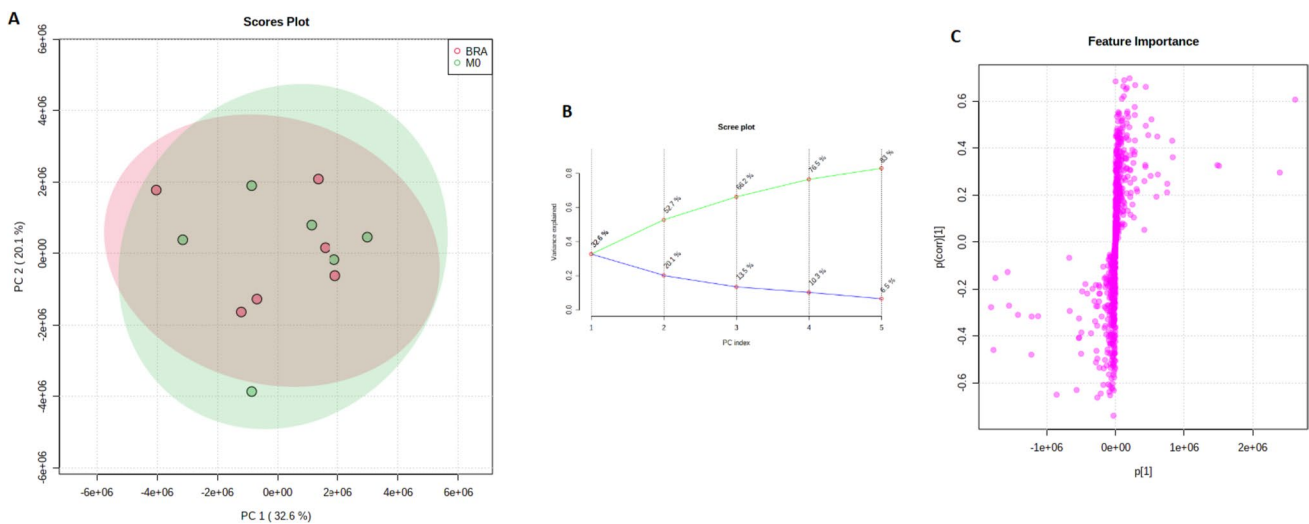


**Fig. 1** **A** showing PCA Scores plot between the PCs is pairwise providing an overview of the various separation patterns among the significant PCs. The explained variances are shown in brackets. **B** is the Scree plot showing the variances explained by the calculated PCs. Scree plot shows the variance explained by PCs. The green line on

top shows the accumulated variance explained; the blue line underneath shows the variance explained by individual PC. **C** delineates S-plot showing the variable importance in a model, combining the covariance and the correlation (p(corr)) loading profile. (Color figure online)

**Analysis of differentially expressed gens: BRA vs. M0**

Based on previous results from multivariate statistics, the Student’s T-test was applied to elucidate for potential genes that were significantly different between the BRA and M0 tissue samples ( $p < 0.05$ , Benjamini–Hochberg false discovery rate). Here 12 genes have been identified with a significant difference between the two groups based on their individual relative expression. The characterization of these genes is described in Fig. 2 and Table 3. Further analysis continued with only these detected genes. Within the twelve significantly different genes, five genes correlate negatively with BRA while seven correlate positive with BRA as shown in Fig. 3.

**Correlation of differentially expressed genes**

To elucidate a potential correlation between significantly different expressed genes and the cohorts at hand, a Heatmap containing the expression of the respective genes has been performed. Horizontal and vertical columns display relative expression of each gene delineating the correlation between the genes. Each bar in the columns represents the expression intensity. For example, the blue scale indicates a decreased level, while the red scale indicates an increased level. The dendrogram on the left was codirected based on the genetic intensity expression profiles (Fig. 4A). Moreover, in the next step (Fig. 4B) an investigation of potential correlation between identified genes and both patient groups

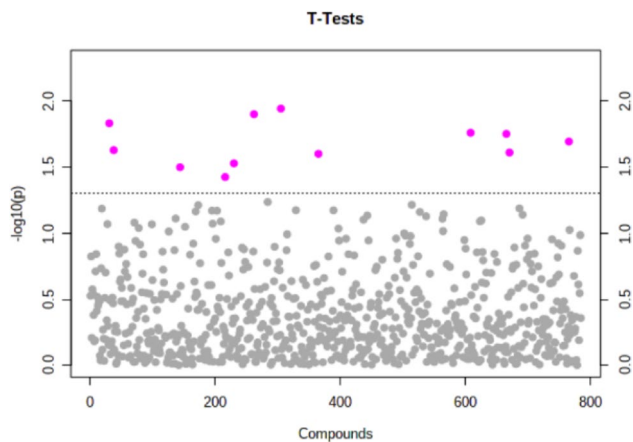


**Fig. 2** Shows identified five features correlating positively and seven features correlating negatively with the corresponding PCs

**Table 3** A shows the important features identified by t-tests

Gene	t. stat	p-value	FDR
ALB	-2,94	0.014	0.985
RBX1	-2,84	0.017	0.985
TGFBR2	-2,64	0.025	0.985
EP300	-2,39	0.038	0.985
TFDP1	-2,83	0.017	0.985
ERMP1	2,53	0.029	0.985
KISS1	2,63	0.025	0.985
TRIM39	2,76	0.02	0.985
NME4	2,51	0.03	0.985
RAB25	2,39	0.037	0.985
SLPI	2,84	0.017	0.985
GDF6	2,29	0.044	0.985

Important features selected by t-tests with threshold 0.05. Purple circles represent features above the threshold. Note the p values are transformed by  $-\log_{10}$  so that the more significant features (with smaller p values) will be plotted higher on the graph. **B** includes statistical characteristics of the 12 identified genes

were performed. Here the gene expression profile accurately reflects the discrimination of the cohort M0 and BRA without prior codirection. The five previously identified genes, which are increased in BRA group and load on TGF $\beta$  pathway have been shown to correlate within each other. Also, a correlating antecedence of TGFBR2, ALB and EP300 for the BRA group appears to reveal as well.

### Principal component analysis focusing on differential gene expression profiles

As a PCA with 770 genes failed to separate the BRA group from the M0 group, the same method was applied with the significantly different genes as shown in Fig. 5. The second

PCA with twelve genes distinguished the cohort into two separate groups. Kaiser–Meyer–Olkin Measure of Sampling Adequacy (KMO = 0.841 and Chi-quadrat (120) = 721,  $p < 0.02$ ) betokens validity of the calculated principal component analysis. Principal component 1 explains 50% of variance. PC2 explains 30.8% of variance in given calculation. Thus, a more than satisfying distinction between both cohorts has been achieved. Corresponding Scree plot shows two PCs with an Eigenvalue  $> 1$ . A distinct elbow spot after PC2 indicates certainty of further analysis as a two-factor analysis. In a S-plot, the predefined genes have been confirmed to be characterized with high correlation and covariance with the separation of the cohort into the clinically different groups. Interestingly, the characterization of the twelve significantly different genes on their corresponding principal component delineates an inhomogeneous allocation of loading on each component.

Despite the correlation of above mentioned differentially expressed genes, functional gene groups have been characterized by specific loadings of each gen on the principal components using the Cohen loading as a cut off, where larger than 0.5 is assumed as strong loading [14]. In respect to the identified genes, ALB, TGFBR2, RBX1, TFDP1 and EP300 exhibited critically positive or negative loading on principal component 1. In comparison, three genes have shown clear positive loading on principal component 2. Nonetheless, with given results from PC1 explaining more than 50% of the variance between both groups, more detailed investigation of PC1 and its functional group of genes by pathway analysis was indicated. Loading are summarized in Table 4.

## GSEA analysis

### Tested databases and pathways

The set of genes identified with the NanoString analysis were further evaluated by GSEA. This pathway analysis, as usual, considered the complete set of genes without regard to single gene expression values. Furthermore, GSEA and NanoString results were compared to several commonly available databases namely Biocarta, Gene Ontology (GO), Reactome, Kyoto Encyclopedia of Genes and Genomes (KEGG), Hallmark gene sets, oncogenic and immunologic signatures. Each database, the total number of potential pathways of each database as well as the number of tested pathways are described in Table 4.

GSEA was applied to compare M0 and BRA group to display potential profiles of both groups and herewith delineate risk profiles. Several pathways proved to be significantly different expressed between both groups BRA and M0 (Table 5). To further elucidate on important genes influencing the process of

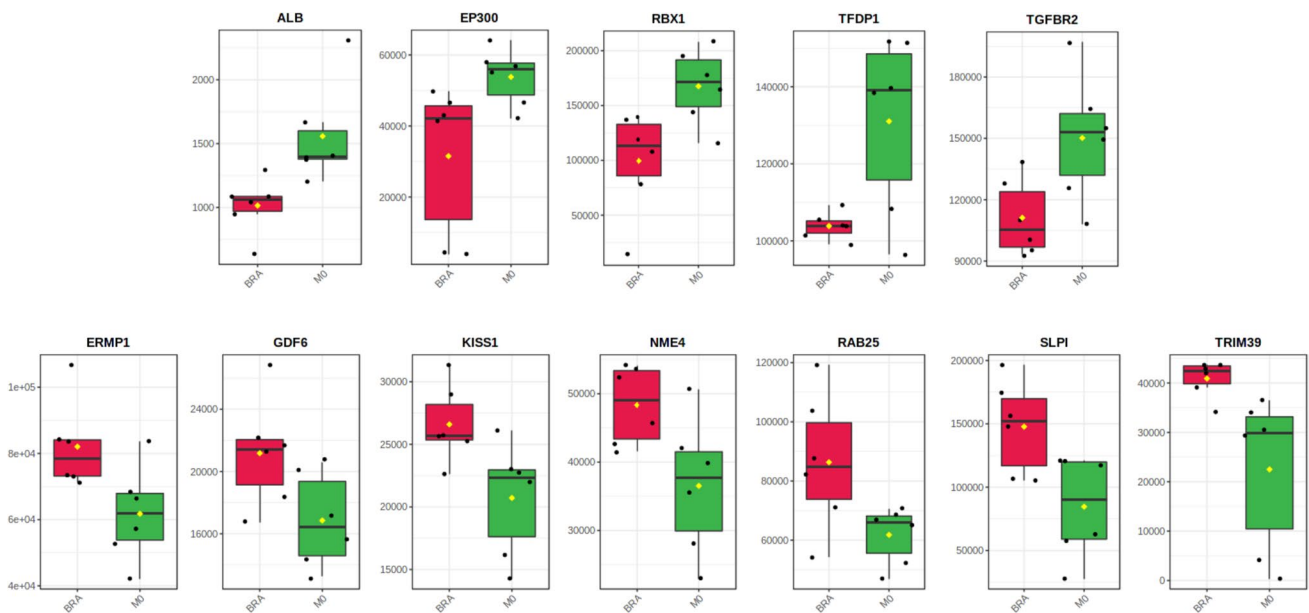


**Fig. 3** Shows identified five features correlating positively and seven features correlating negatively with the corresponding PCs

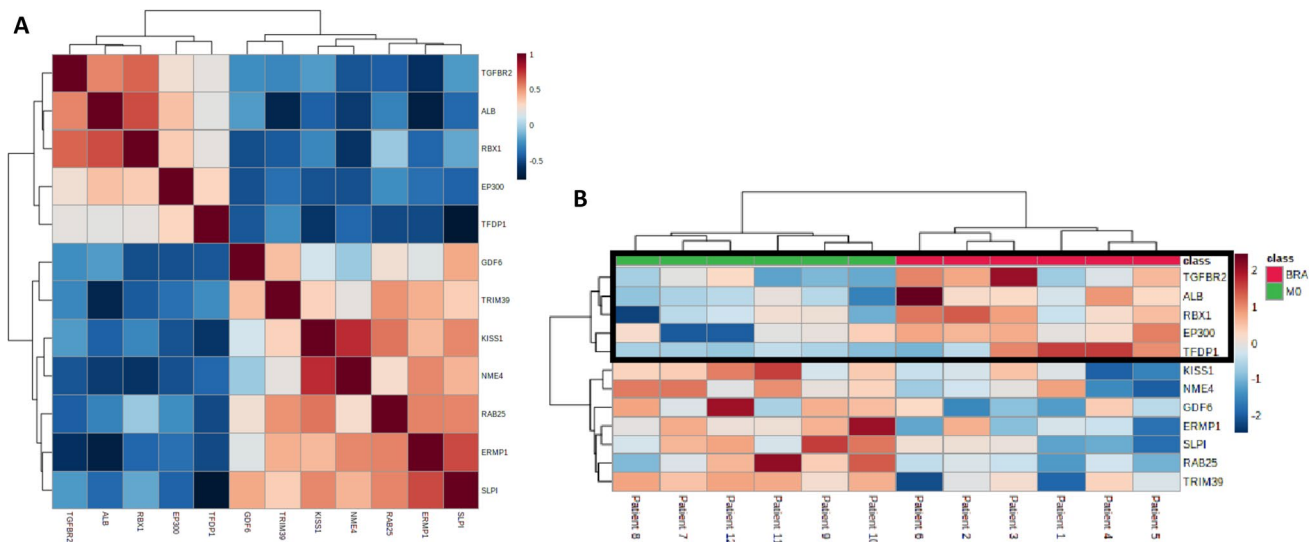


**Fig. 4** **A** shows the clustering result in the form of a heatmap. **B** overall correlation heatmap between the significant genes and the cohort with-out prior clustering

brain metastases, we cross-referenced the high-risk gene set of this analysis with all significantly different expressed pathways (Table 6). Of those, all genes critically loading on PC1 also play a role in the TGFβ-pathway. The TGFβ-pathway itself proved to be significantly different expressed using not only the Hallmarks (Fig. 6) but also the KEGG (Fig. 7) pathway database (normalized enrichment score (NES) = -1.5,  $p < 0.04$ ,  $q = 0.20$ ; NES = -1.7,  $p < 0.04$ ,  $q = 0.16$  respectively). Of those 5 genes loading on PC1, four genes, namely TGFβR2, TFDPI, RBX1, and EP300 even contributed to the core enrichment

score of the TGFβ-pathway indicating a major influence on its functioning. Thus, in tumours leading to brain metastases (BRA) compared to M0, the TGFβ signalling is significantly dysregulated.

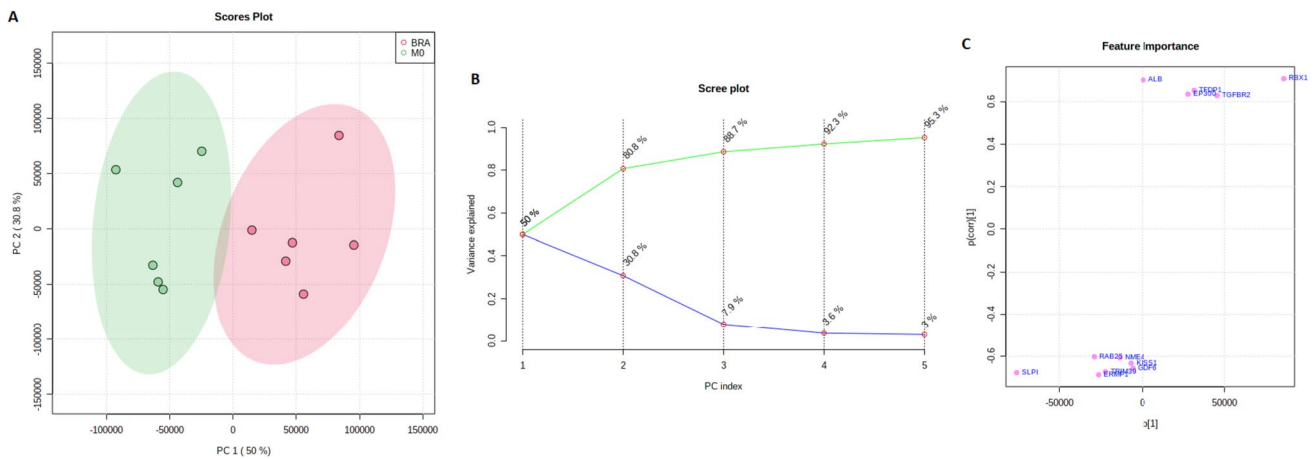


**Fig. 5** **A** visualizes PCA Scores plot between the PCs is pairwise providing an overview of the various separation patterns among the significant PCs. The explained variances are shown in brackets. **B** depicts the Scree plot showing the variances explained by the calculated PCs. Scree plot shows the variance explained by PCs. The

green line on top shows the accumulated variance explained; the blue line underneath shows the variance explained by individual PC. **C** displays PCA loadings S-plot showing the variable importance in a model, combining the covariance and the correlation ( $p(\text{corr})$ ). (Color figure online)

**Table 4** Shows the loading of identified significant features on PC1 and PC2

Gene	Loading PC1	Loading PC2
ALB	.85	-.2
RBX1	.82	-.27
TGFBR2	.73	-.22
EP300	-.71	.12
TFDP1	.58	-.59
ERMP1	-.39	.85
KISS1	-.05	.79
TRIM39	-.33	.76
NME4	-.04	-.23
RAB25	-.17	.18
SLPI	-.07	.13
GDF6	-.14	0

Green and red marks strong (> .5) in cohan scale

## Discussion

Recently, research of distant metastases in CRC patients increased exponentially. A number of studies has already investigated hepatic, peritoneal, pulmonary as well as continuing distant metastases in colorectal cancer [5, 15]. Yet, with respect to tumor biology and brain metastases, little is known so far.

The aim of this work was to analyse genetic differences and commonalities between patients without distant metastases and patients with brain metastases from colorectal adenocarcinoma. Therefore, RNA NanoString-Analysis was applied. We elucidated on comparative differences

in the genetical profiles of M0 and BRA tumour tissues by using an unsupervised principal component analysis (PCA). The final PCA was performed using the complete set of significantly different expressed genes between M0 and BRA. We were able to determine a gene signature that provides a sophisticated group separation between M0 and BRA (Fig. 4). The consecutive scree- and S-plots in Fig. 4 confirm this analysis. Moreover, the scree-plot suggested that only PC1 was able to explain more that 50% of the variance between BRA and M0. The unsupervised heat map in Fig. 5B illustrates a clear cluster pattern dividing M0 from BRA. All genes with strong loading characteristics on PC1 were therefor cross-referenced with the subsequently performed accurate gene set enrichment analysis (GSEA). The GSEA revealed a clear dysregulation of the TGFβ pathway in compared cohorts M0 and BRA (Figs. 6 and 7). Interestingly, the targeted pathways analysis of the identified genes confirmed that in fact almost all strong loading genes of PC1, namely ALB, RBX1, TGFBR2, EP300 and TFDP1, play a role in the TGFβ pathway suggesting the TGFβ pathway as a crucial player in the development of brain metastases in primary CRC.

The TGFβ pathway signalling pathway is said to have a paradox influence on tumour progression and metastases, a fact well known as the TGFβ paradox. Recent literature argues that physiological TGFβ upregulation triggers induction of apoptosis and proliferation as well as cell cycle arrest in early stage cancer cells [16, 17]. In healthy tissue likewise, TGFβ inhibits epidermal growth and cell transition and thus shows an anti-tumour effects. These results are supported by Bakir et al. 2020, who argue that a TGFβ-R2 deficiency, a core TGFβ pathway regulator, leads to increased

**Table 5** Tested databases and pathways

Database	Potential pathways (n)	Tested pathways (n)	n	p-value	q-value
Reactome pathways	674	58			
INNATE IMMUNE SYSTEM			26	0.014	0.22
KEGG pathways	186	57			
CHEMOKINE SIGNALING			45	0.014	0.21
NOD LIKE RECEPTOR SIGNALING			16	0.024	0.17
TGF BETA SIGNALING			60	0.043	0.17
LEISHMANIA INFECTION			21	0.025	0.19
WNT SIGNALING			35	0.058	0.21
COLORECTAL CANCER			30	0.057	0.23
ADHERENS JUNCTION			25	0.11	0.21
Hallmarks pathways	50	24			
INTERFERON GAMMA_RESPONSE			26	<0.001	0.16
ALLOGRAFT REJECTION			41	0.002	0.094
TGF BETA SIGNALING			19	0.046	0.21
Biocarta	217	14			
ALK			16	0.039	0.21
MAPK			19	0.024	0.14
PPARA			18	0.045	0.20
CTCF			15	0.09	0.23
BIOPEPTIDES			16	0.12	0.24
Immunologic signatures	4872	1177			
GSE29618			15	<0.001	0.21
GSE9988			20	<0.001	0.22
GSE43863			16	0.01	0.17
GSE8685			16	0.004	0.19
GSE12366			19	0.004	0.18

**Table 6** significant genes and significant pathways

Gene/Pathway	ALK	CTCF	PPAR $\alpha$	AT1	GC	AJ	CRC	TGF $\beta$	WNTS	IIS
ALB										
EP300			X			X		X	X	X
RBX1								X	X	
TFDP1								X		
TGFBR2	X	X		X	X	X	X	X		X

Genes involved in corresponding pathways marked with X

inflammatory burden and tumor progression via higher levels of tumor necrosis factor- $\alpha$  (TNF- $\alpha$ ), interleukin (IL)-8 and interferon (IFN)- $\gamma$  [17]. These findings might directly explain the observed overregulation of the TGF $\beta$  pathway in our M0 cohort. This might underline that under certain circumstances, the TGF $\beta$  pathway might inhibit metastatic potential. Further, the TGFBR2 gene is downregulated in BRA in our gene expression analysis. This result is supported by its negative loading on PC1 in the principal component analysis of this stud. Li et al. 2017 highlighted a direct link to our findings by real-time PCR results in non-small cell lung cancer tissue. They could indeed correlate a repression of TGFBR2 with more distant metastases and tumor growth [18].

TGF $\beta$  inactivation in malignant colon cells has also proved to boost malignant potential via the MAPK and Wnt- $\beta$ -catenin pathway [19]. Even after curative resection, a disruption in TGF- $\beta$  signaling results in a much more progressive phenotype thus limiting patient prognosis [20]. Notably, these results have been shown to be true especially for advanced cancer stages. The fact that in our cohort, overrepresentation of the TGF $\beta$  signalling might act preventive regarding brain metastases might serve as new insights as to how TGF $\beta$  signalling influences tumor behaviour.

Contrary to these findings, others argue that even in low-stage cancer cells, TGF $\beta$  can induce tumour progression. While this assumption does not contradict our findings, it supports the above mentioned TGF $\beta$  paradox. Additionally,



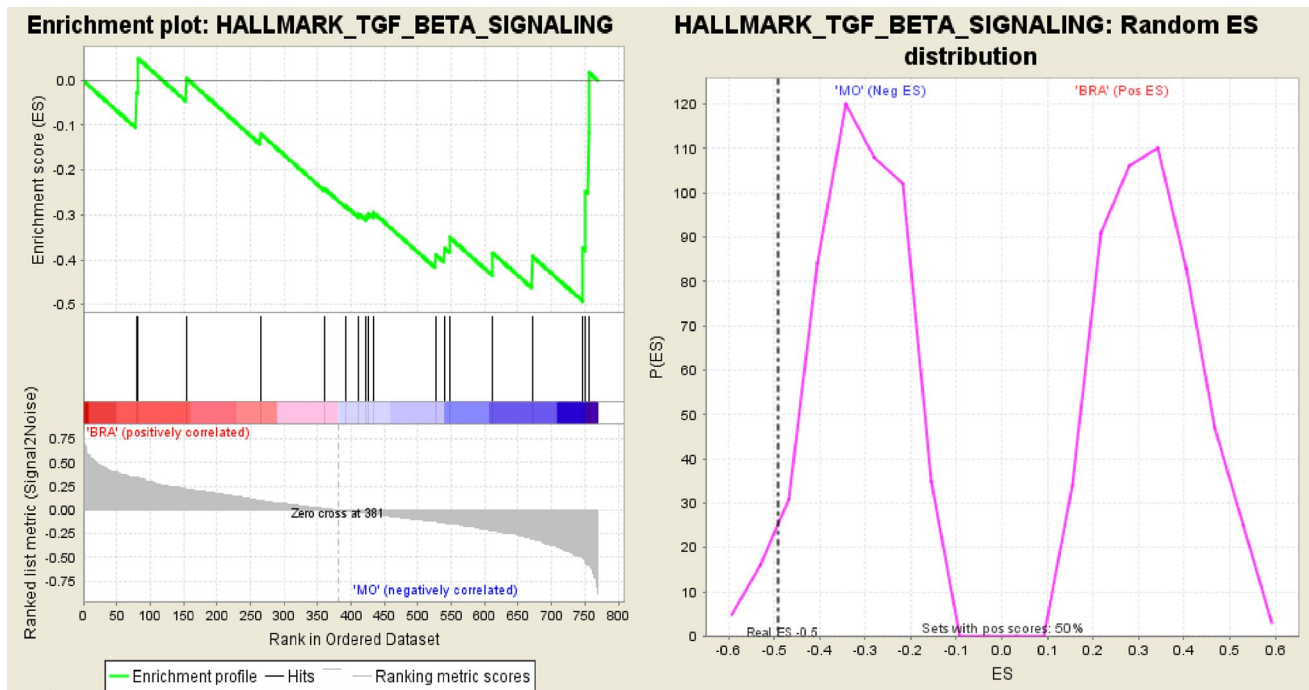


**Fig. 6** Enrichment plot for the TGFβ signalling pathway from Hallmark database. Here the enrichment curve indicates a significant alteration in comparison to the M0 group

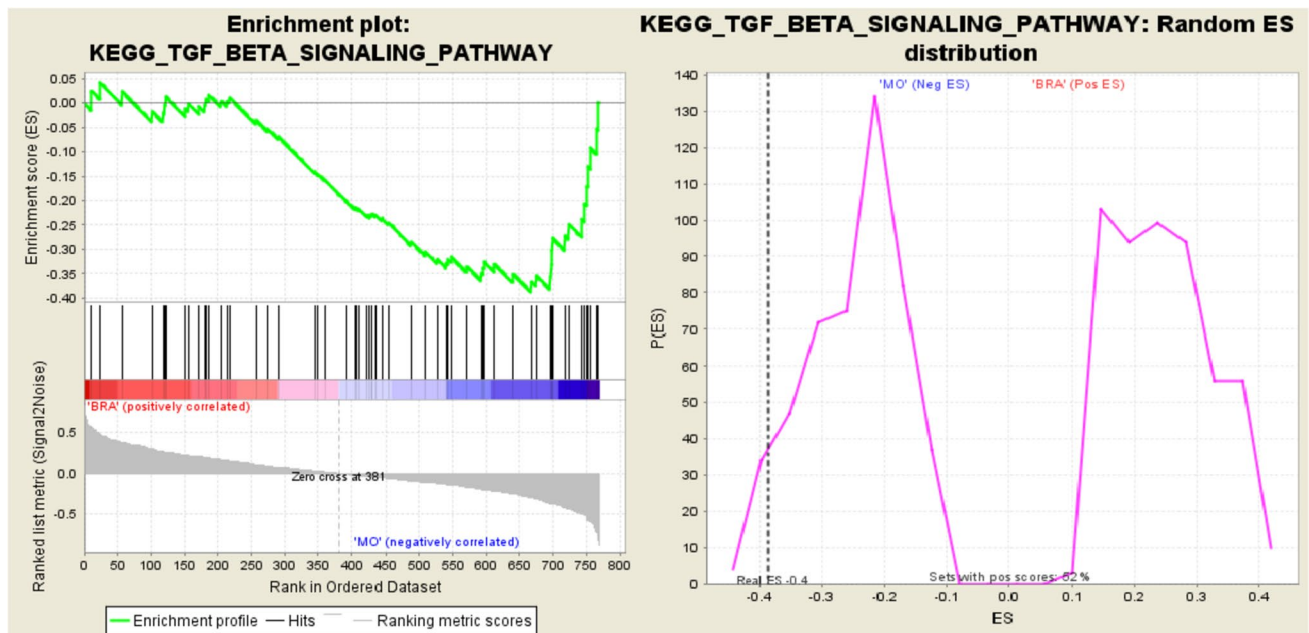


**Fig. 7** Enrichment plot for the TGFβ signalling pathway from Hallmark database. Here the enrichment curve indicates a significant alteration in comparison to the M0 group

this paradox states that in later stage cancer types, the opposite such as genomic instability and immune evasion as well as tumorigenic alterations in peritumoral stroma cells is possible. In that context, the TGF-β pathway is associated

with changes in Erk, MAPK and SMAD signaling [16]. Contradictory to that, however, are the finding of Bacman et al. 2007. They state that a loss of key regulators of the TGFβ pathway, TGFβ-R1 and R2, results in increased lymph

node metastases and shorter survival rates [21]. They further mention that peritumoral stromal TGF- $\beta$  R2 even serve as an independent prognostic marker for survival. These results are supported by Hussain et al. 2018. Their hypothesis was that higher levels of TGF $\beta$  dependent IL-23 lead to less macrophage associated metastases in pancreatic cancer [22]. They therefore injected NGS mice with IL-23, macrophages and TGF $\beta$  and could observe less metastatic potential and higher levels of IL-23, macrophages and TGF $\beta$  in the long-term survivor group [22]. Even stronger in line with our finding that at least parts of the TGF $\beta$  pathway prevent brain metastases are the results of Okita et al. 2018. While they confirm that TGF $\beta$ -signalling mutations might enhance EMT and metastases in some CRC patients, they point out other subtypes in which TGF- $\beta$ R2 actively hinders EMT and metastases thus leading to a better prognosis [2]. It seems very interesting to further elucidate on those subtypes regarding brain metastases and TGF $\beta$  pathway expressions.

The context dependent, by times paradox biological implications within the TGF $\beta$  pathway ask for further investigation. It is still unclear why this pathway can enhance and hinder tumor progression in the same type of cancer. While we could point out that the TGF $\beta$  signalling might reduce brain metastases, above mentioned research can also indicate that it can just as well lead to more metastatic potential. A question which again can be summed up as the paradox functioning of the TGF $\beta$  pathway. Taken together the demonstrated results and pre-existing evidence, specific mutations as well as up or downregulations in the TGF $\beta$  pathway have been re-assessed to influence the development of distant metastases in the central nervous system. Undoubtedly, further elucidation on why and how the process of brain metastases is influenced by the TGF $\beta$  pathway is required. More so because it remains unclear which regulating genes play a core role in the biologically complex network facilitating brain metastases. Patient survival can shrink down to 2–10 months after the development of brain metastases. Further, the gold standard for brain metastases detection is still the MRI, notably not a routine diagnostic, complex and costly. We therefore think that our research can be an efficient starting point to elucidate on gene signatures and biomarkers for early detection of brain metastases.

**Author contributions** Authors' contribution: SJ: Took part in study design and coordination, tissue selection, validation and evaluation of immunohistochemistry, performed statistical tests and drafted the manuscript. CH: Took part in study design and coordination, tissue selection, prepared figures. MM: Processed primary RNA, analyzed and calculated NanoString data, performed statistical analysis. JK: Took part in study design and coordination, tissue selection, processed primary RNA, analyzed and calculated NanoString data, performed statistical analysis. TK: Conceived of the study, provided funding and helped in its design. JW: Conceived of the study, provided funding and

helped in its design. MKA: Conceived of the study, provided funding and helped in its design and coordination, drafted the manuscript. JN: Conceived of the study, provided funding and helped in its design and coordination, participated in tissue selection, validation and evaluation of immunohistochemistry, drafted the manuscript. COI/ Disclosures: The authors have no related conflicts of interest to declare. No external is to declare.

**Funding** Open Access funding enabled and organized by Projekt DEAL.

## Declarations

**Conflict of interests** This work has not been published or accepted for publication, nor is it under consideration at another journal. Moreover, I would like to declare on behalf of the authors that there are no ethical nor other conflicts of interests and that all authors have seen and approved the manuscript.

**Ethical approval** The study was performed according to the recommendations of the local ethics committee of the Medical Faculty of the LMU Munich who approved the protocol of the study (no. 19-966).

**Open Access** This article is licensed under a Creative Commons Attribution 4.0 International License, which permits use, sharing, adaptation, distribution and reproduction in any medium or format, as long as you give appropriate credit to the original author(s) and the source, provide a link to the Creative Commons licence, and indicate if changes were made. The images or other third party material in this article are included in the article's Creative Commons licence, unless indicated otherwise in a credit line to the material. If material is not included in the article's Creative Commons licence and your intended use is not permitted by statutory regulation or exceeds the permitted use, you will need to obtain permission directly from the copyright holder. To view a copy of this licence, visit <http://creativecommons.org/licenses/by/4.0/>.

## References

1. Muller S, Kohler F, Hendricks A et al (2021) Brain metastases from colorectal cancer: a systematic review of the literature and meta-analysis to establish a guideline for daily treatment. *Cancers* (Basel). 13:900
2. Okita A, Takahashi S, Ouchi K et al (2018) Consensus molecular subtypes classification of colorectal cancer as a predictive factor for chemotherapeutic efficacy against metastatic colorectal cancer. *Oncotarget* 9:18698–18711
3. Thurmaier J, Heinemann V, Engel J et al (2021) Patients with colorectal cancer and brain metastasis: the relevance of extracranial metastatic patterns predicting time intervals to first occurrence of intracranial metastasis and survival. *Int J Cancer* 148:1919–1927
4. Mege D, Sans A, Ouaisi M, Iannelli A, Sielezneff I (2018) Brain metastases from colorectal cancer: characteristics and management. *ANZ J Surg* 88:140–145
5. Jacob S, Bosch F, Schoenberg MB et al (2021) Expression of CIB1 correlates with colorectal liver metastases but not with peritoneal carcinomatosis. *BMC Cancer* 21:1243
6. Jacob S, Jurinovic V, Lampert C et al (2021) The association of immunosurveillance and distant metastases in colorectal cancer. *J Cancer Res Clin Oncol* 147:3333–3341

7. Sun J, Wang C, Zhang Y et al (2019) Genomic signatures reveal DNA damage response deficiency in colorectal cancer brain metastases. *Nat Commun* 10:3190
8. Wang R, Zhu Y, Liu X, Liao X, He J, Niu L (2019) The Clinicopathological features and survival outcomes of patients with different metastatic sites in stage IV breast cancer. *BMC Cancer* 19:1091
9. Cheng Y, Zhang X, Wang Z, Wang J (2020) Reconstruction of immune microenvironment and signaling pathways in endometrioid endometrial adenocarcinoma during formation of lymphovascular space involvement and lymph node metastasis. *Front Oncol* 10:595082
10. Sundar R, Liu DH, Hutchins GG et al (2020) Spatial profiling of gastric cancer patient-matched primary and locoregional metastases reveals principles of tumour dissemination. *Gut*. <https://doi.org/10.1136/gutjnl-2020-320805>
11. Fabregat A, Jupe S, Matthews L et al (2018) The reactome pathway knowledgebase. *Nucleic Acids Res* 46:D649-d655
12. Kanehisa M, Furumichi M, Tanabe M, Sato Y, Morishima K (2017) KEGG: new perspectives on genomes, pathways, diseases and drugs. *Nucleic Acids Res* 45:D353-d361
13. Liberzon A, Birger C, Thorvaldsdóttir H, Ghandi M, Mesirov JP, Tamayo P (2015) The molecular signatures database (MSigDB) hallmark gene set collection. *Cell Syst* 1:417–425
14. Cohen J (1992) A power primer. *Psychol Bull* 112:155–159
15. Pretzsch E, Bosch F, Neumann J et al (2019) Mechanisms of metastasis in colorectal cancer and metastatic organotropism: hematogenous versus peritoneal spread. *J Oncol* 2019:7407190
16. Seoane J, Gomis RR (2017) TGF- $\beta$  family signaling in tumor suppression and cancer progression. *Cold Spring Harb Perspect Biol*. 9:a022277
17. Wu F, Weigel KJ, Zhou H, Wang XJ (2018) Paradoxical roles of TGF- $\beta$  signaling in suppressing and promoting squamous cell carcinoma. *Acta Biochim Biophys Sin (Shanghai)* 50:98–105
18. Li G, Wu F, Yang H, Deng X, Yuan Y (2017) MiR-9-5p promotes cell growth and metastasis in non-small cell lung cancer through the repression of TGFBR2. *Biomed Pharmacother* 96:1170–1178
19. Morris SM, Davison J, Carter KT et al (2017) Transposon mutagenesis identifies candidate genes that cooperate with loss of transforming growth factor-beta signaling in mouse intestinal neoplasms. *Int J Cancer* 140:853–863
20. Roth AD, Delorenzi M, Tejpar S et al (2012) Integrated analysis of molecular and clinical prognostic factors in stage II/III colon cancer. *J Natl Cancer Inst* 104:1635–1646
21. Bacman D, Merkel S, Croner R, Papadopoulos T, Brueckl W, Dimmler A (2007) TGF-beta receptor 2 downregulation in tumour-associated stroma worsens prognosis and high-grade tumours show more tumour-associated macrophages and lower TGF-beta1 expression in colon carcinoma: a retrospective study. *BMC Cancer* 7:156
22. Hussain SM, Reed LF, Krasnick BA et al (2018) IL23 and TGF- $\beta$  diminish macrophage associated metastasis in pancreatic carcinoma. *Sci Rep* 8:5808

**Publisher's Note** Springer Nature remains neutral with regard to jurisdictional claims in published maps and institutional affiliations.